Supplemental Information for:

Intrinsic Intertlayer Electric Field Induced Switched Regulatory Mechanisms of Photovoltaics and Photocatalysis in Z-scheme Heterobilayers

Qiang Wang,[a] Keying Han,*[,a] Yan Liang,[b] Xingshuai Lv,[c] Thomas Frauenheim,[d] Xiangrong Meng,[a] Sheng Wang,[a] Defeng Guo,*[,a] and Bin Wang*[,e]

[a] State Key Laboratory of Metastable Materials Science and Technology and Key Laboratory for Microstructural Material Physics of Hebei Province, School of Science, Yanshan University, Qinhuangdao 066004, People's Republic of China. E-mail: hanky@stumail.ysu.edu.cn; guodf@ysu.edu.cn

[b] College of Physics and Optoelectronic Engineering, Faculty of Information Science and Engineering, Ocean University of China, Songling Road 238, Qingdao 266100, People's Republic of China.

[c] College of Chemistry and Chemical Engineering, Ocean University of China, Songling Road 238, Qingdao 266100, People's Republic of China.

[d] School of Science, Constructor University, 28759 Bremen, Germany; Computational Science and Applied Research Institute (CSAR), Shenzhen518110, P. R. China; Beijing Computational Science Research Center (CSRC), Beijing 100193, P. R. China.

[e] Shenzhen Key Laboratory of Advanced Thin Films and Applications, College of Physics and Optoelectronic Engineering, Shenzhen University, Shenzhen, 518060, People's Republic of China. E-mail: binwang@szu.edu.cn

Corresponding Authors:

*E-mail: hanky@stumail.ysu.edu.cn; guodf@ysu.edu.cn

binwang@szu.edu.cn

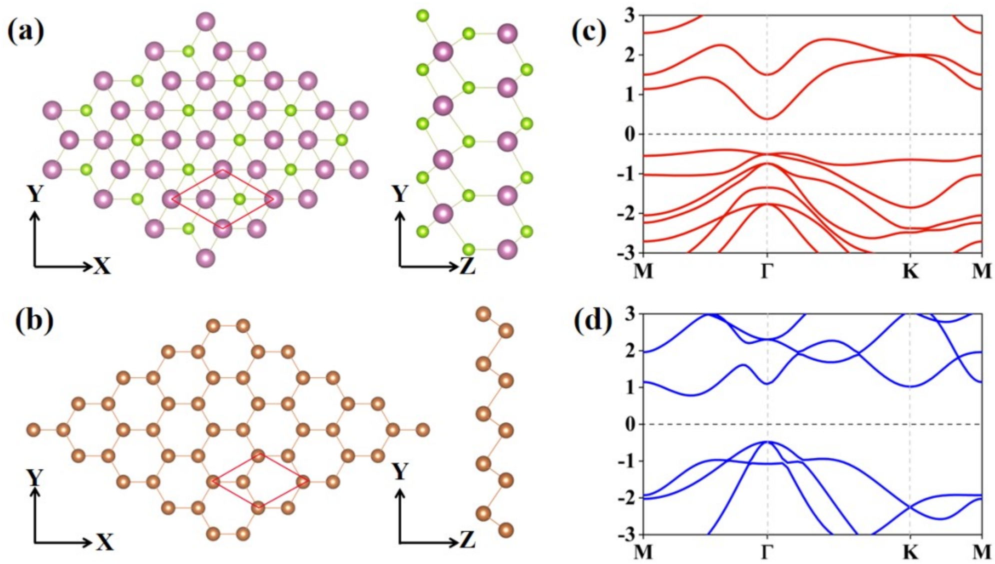

Fig. S1. (a-b) Top and side views of schematic structures for In_2Se_3 and Sb monolayer, respectively. (c-d) Band structures of In_2Se_3 and Sb monolayer based on PBE level， in each panel, the Fermi levels are marked with horizontal black dashed lines.

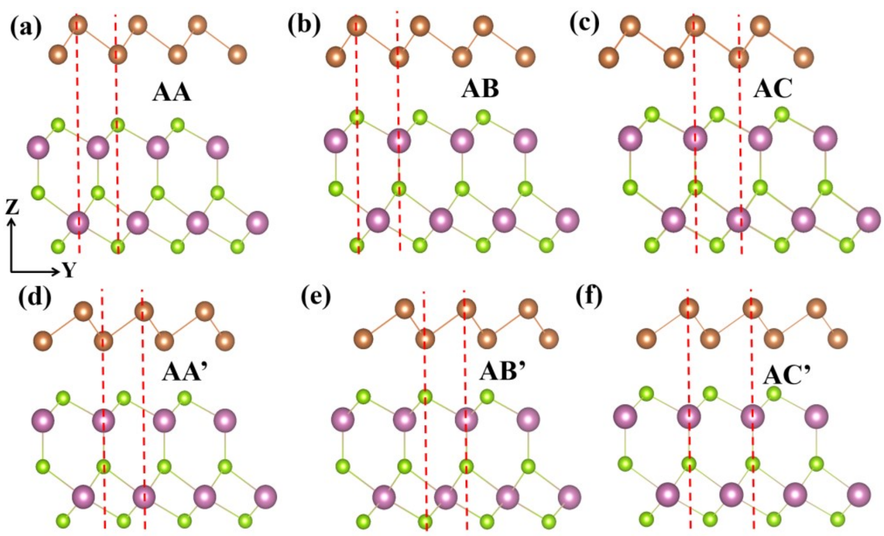

Fig. S2 . (a-f) Side view of different stacking modes for In_2Se_3/Sb vdWH, with the alignment of atoms being marked by red dotted lines.

TABLE SI. Total energies (E_{tot}) of In_2Se_3/Sb vdWH under different stacking modes.

Stacking	AA	AB	AC	AA’	AB’	AC’
E_{tot}(eV)	-27.3817	-27.4833	-27.4916	-27.4817	-27.3824	--27.3818

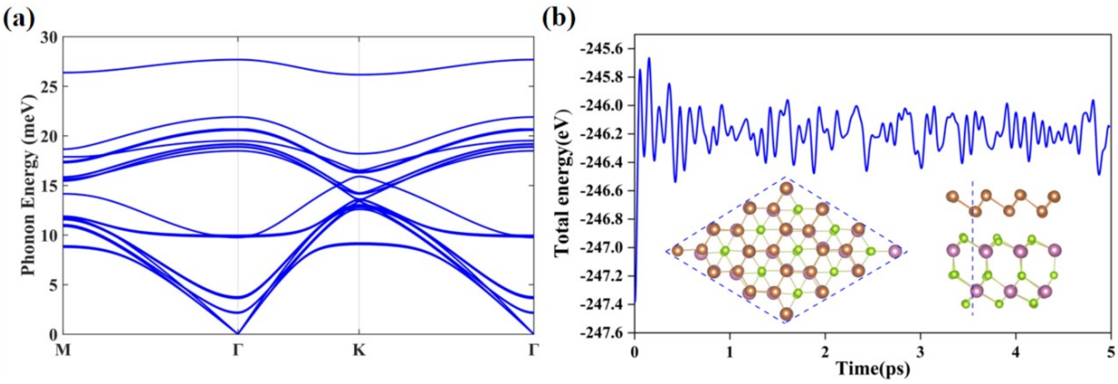

Fig. S3 . (a) Phonon band dispersion curves of In_2Se_3/Sb vdWH. (b) The variation in total energy of the 3×3 In_2Se_3/Sb vdWH supercell as a function of time under 300 K. Insets: top and side views of snapshot for the vdWH after evolution of 5 ps.

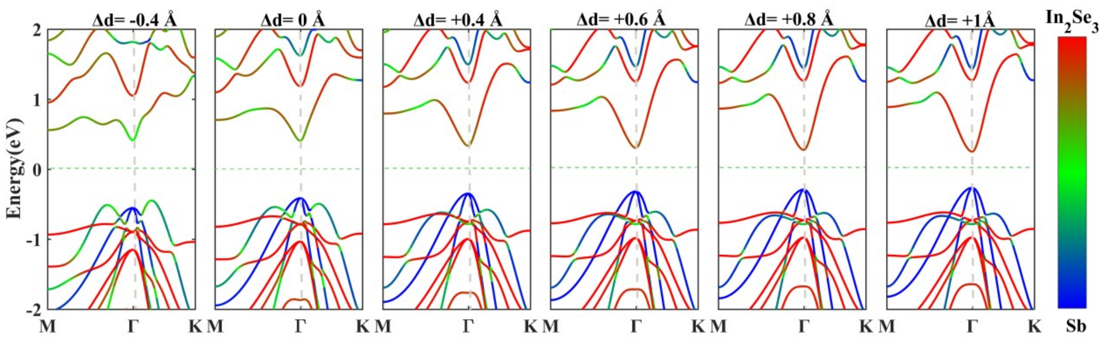

Fig. S4 . Band structures of In_2Se_3/Sb vdWH under various interlayer distances d at PBE level. In each panel, the energy bands projected on In_2Se_3 and Sb components are colored in red and blue, respectively; The Fermi levels are marked with horizontal green dashed lines; and the negative/positive sign indicates corresponding decrease/increase of d.

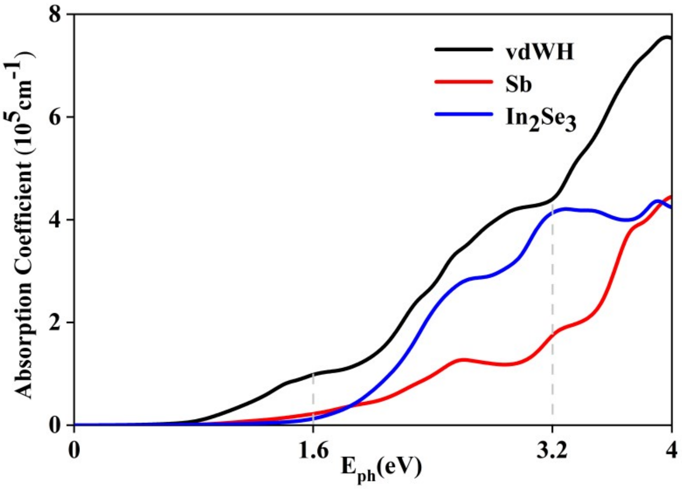

Fig. S5 . Optical absorption coefficients versus incident light energy for monolayer In_2Se_3, Sb and In_2Se_3/Sb vdWH at PBE level.

Solar-to-hydrogen (STH) efficiency for Z-scheme vdWH

Regarding the cacculation method of solar-to-hydrogen (STH) efficiency is defined as follows:

$$\eta_{STH} = \eta_{abs} \times \eta_{cu} \tag{1}$$

where η_{abs} and η_{cu} are the efficiency of light absorption and carrier utilization, respectively, in which η_{abs} is estimated by:

$$\eta_{abs} = \frac{\int_{E_g}^{\infty} P(\hbar\omega) d(\hbar\omega)}{\int_{0}^{\infty} P(\hbar\omega) d(\hbar\omega)} \tag{2}$$

where $P(\hbar\omega)$ is the solar flux at AM1.5 photon energy $\hbar\omega$ and E_g is the band gap of the material.

According to Ref.[1,2,3], only half of the photo-generated carriers can be converted to hydrogen energy in Z-scheme photocatalytic water splitting. The $\eta_{cu}$is defined as:

$$\eta_{cu} = 0.5 \times \frac{\Delta G \int_{E}^{\infty} \frac{P(\hbar\omega)}{\hbar\omega} d(\hbar\omega)}{\int_{E_g}^{\infty} P(\hbar\omega) d(\hbar\omega)} \tag{3}$$

where ΔG is the potential difference 1.23 eV for water splitting, and E is the actual photon energy used for water splitting. For a direct Z-scheme vdWH consisting of A and B systems, to achieve the Z-scheme mechanism for water redox reactions, the driving force from photo-generated electrons and holes must enable both the hydrogen evolution reaction (HER) in system A and the oxygen evolution reaction (OER) in system B. E can be estimated by:

$$E = \begin{cases} max(E_{gA,}E_{gB}), & (\chi_{A(H_2)} \geq 0.2, \chi_{B(O_2)} \geq 0.6) \\ max(E_{gA} + 0.2 - \chi_{A(H_2)}, E_{gB}), & (\chi_{A(H_2)} < 0.2, \chi_{B(O_2)} \geq 0.6) \\ max(E_{gA}, E_{gB} + 0.6 - \chi_{B(O_2)}), & (\chi_{A(H_2)} \geq 0.2, \chi_{B(O_2)} < 0.6) \\ max(E_{gA} + 0.2 - \chi_{A(H_2)}, E_{gB} + 0.6 - \chi_{B(O_2)}), & (\chi_{A(H_2)} < 0.2, \chi_{B(O_2)} < 0.6) \end{cases} \tag{4}$$

where $\chi_{A(H_2)}$ and $\chi_{B(O_2)}$ represent the overpotentials for HER in system A and OER in system B, respectively. Considering the energy loss during carrier migration between different materials, the required over potentials for HER and OER are assumed to be 0.2 eV and 0.6 eV, respectively.

In addition, the intrinsic interlayer built-in electric filed does positive work for the electron−hole separation during the process of photocatalytic water splitting. Therefore, this part of work should be added into the total energy, and then the corrected STH efficiency of photocatalytic water splitting for 2D material with intrinsic E_{int} is calculated as:

$$\eta'_{STH} = \eta_{STH} \times \frac{\int_0^\infty P(\hbar\omega)d(\hbar\omega)}{\int_0^\infty P(\hbar\omega)d(\hbar\omega) + \Delta\Phi\int_E^\infty \frac{P(\hbar\omega)}{\hbar\omega}d(\hbar\omega)} \quad (5)$$

where $\Delta\Phi$ is the vacuum level difference on the two single component layers of this 2D In_2Se_3/Sb vdWH.

Reference

1. Y.Fan, J.Wang, M.Zhao, *Nanoscale*, 2019, 11, 14836-14843.
2. G.Wang, J.Chang, W.Tang, W.Xie, Y.Ang, *J Phys D Appl Phys,* 2022, 55, 293002.
3. C.Fu, X.Li, J.Yang, *Chem. Sci.*, 2021, 12, 2863-2869.